International Journal of Thermophysics, Vol. 15, No. 3, 1994

A Comparison of Ideal and Real Moist Air Models for Calculating Humidity Ratio and Relative Humidity in the 213.15 to 473.15 K Range and up to a Pressure of 1 MPa

G. Buonanno,[1] A. A. Carotenuto,[1] L. Crovini,[2] and M. Dell'Isola[1]

Received January 31, 1994

This study evaluates how the ideal mixture model of moist air approximates a real mixture model when determining both humidity ratio and relative humidity for the 0.1- to 1-MPa pressure range and the −60 to 200°C temperature range. The relevant thermodynamic properties are calculated using, among others, a specific algorithm based on the relationships proposed by Hyland and Wexler corrected for the new ITS-90 temperature scale.

KEY WORDS: moist air; real mixture; temperature scale; thermodynamic properties.

1. INTRODUCTION

The accurate determination of the humidity ratio in air, i.e., $w = m_w/m_a$, where m_w and m_a are the mass of water vapor and air, respectively, in a given volume of gas mixture, is required in both scientific and industrial applications. For instance, determinations of w to within ±1% are sought to obtain the density of atmospheric air, which is required in metrological applications such as the air-buoyancy correction in mass measurement and the determination of the air refractive index as required by laser interferometery. Another case is the performance evaluation of air-conditioning components in the aerospace industry.

Additionally, and with particular reference to sorption–desorption processes, it is necessary to determine relative humidity, ϕ, a quantity being

---

[1] Dipartimento de Ingegneria Industriale, Università degli Studi di Cassino, Cassino, Italy.

[2] Istituto di Metrologia "G. Colonetti," Torino, Italy.

defined as the ratio of the actual water-vapor molar fraction to that existing in saturation conditions at the same pressure and temperature. Air humidity can also be expressed as dew-point temperature, T_d, and thermodynamic wet-bulb temperature, T^*. Approximate determinations of ϕ, T_d, and T^* can be carried out with hygroscopic hygrometers. dew-point hygrometers, and psychrometers, respectively. When processing data obtained in such a way, atmospheric air is considered to be a binary mixture of water vapor and dry air, attributing to the latter the conventional chemical composition proposed by Harrison [1]. In the case of ambient air-conditioning plants, the total pressure is generally kept to near 0.1 MPa and the temperature between 0 and 50°C.

Threlked [2] estimated the degree of approximation of an ideal-gas mixture approach under these conditions with respect to the real-gas mixture approach, finding differences not exceeding 0.7% in the calculated relative humidity, enthalpy, and volume of saturated air for the −50 to 50°C temperature range. Furthermore, Nelson and Pate [3] calculated the values at atmospheric pressure of the volume and of both the specific enthalphy and entropy in relation to both the humidity ratio and the relative humidity, for temperatures from −40 to 60°C. There are, however, other applications for conditioning moist air in industrial processes at different pressures and temperatures [4].

The present study evaluates the approximation of the ideal-mixture model compared with a real-mixture model in the 0.1- to 1-MPa pressure and −60 to 200°C temperature ranges, respectively.

This approximation is evaluated for variable thermodynamic conditions using a specific algorithm based on the studies of Hyland and Wexler [5, 6] for a real mixture and on known thermodynamic relationships for an ideal mixture [7].

All the coefficients of the thermodynamic relationships proposed by Hyland and Wexler [5, 6] have been suitably corrected on the basis of the new ITS-90 temperature scale [8].

2. CALCULATION METHOD

The relevant thermodynamic relationships, as investigated in a previous work [9], exhibit the following functional bonds:

(A) $w = w(P, T, \phi)$, (B) $w = w(P, T_d)$, (C) $w = w(P, T, T^*)$

(D) $\phi = \phi(P, T, w)$, (E) $\phi = \phi(P, T, T_d)$, ((F) $\phi = \phi(P, T, T^*)$)

Relationships C and F, however, are of very limited practical use unless the measured wet-bulb temperature is a good approximation of the thermodynamic wet bulb temperature, a condition seldom realized with ordinary psychrometers.

The use of a special algorithm, termed AIR, enables the values of ϕ and w to be calculated using the six relationships outlined above with variable input parameters. The parameters of both the real-gas mixture (ϕ_r, w_r) and the ideal-gas mixture (ϕ_i, w_i) are determined, whence the relative differences are calculated as follows:

$$s_\phi = \frac{\phi_r - \phi_{id}}{\phi_r} \times 100, \qquad s_w = \frac{w_r - w_{id}}{w_r} \times 100 \tag{1}$$

2.1. Calculation of $w = w(P, T, \phi)$

For the ideal-mixture model, we have

$$w_i = \frac{M_w}{M_a} \frac{\phi p_{ws}(T)}{P - \phi p_{ws}(T)} \tag{2}$$

where $M_w = 18.01528\ \text{g} \cdot \text{mol}^{-1}$ and $M_a = 287.9645\ \text{g} \cdot \text{mol}^{-1}$ are the molecular weights of water and dry air, respectively [1], and p_{ws} is the water saturation pressure given by Hyland and Wexler [5], when corrected to account for the ITS-90, namely, for $273.16 \leqslant T \leqslant 473.15$ K (liquid–vapor saturation conditions),

$$\ln(p_{ws}) = \sum_{i=-1}^{3} g_i T^i + g_4 \ln(T) \tag{3}$$

and for $173.16 \leqslant T \leqslant 273.16$ K (ice–vapor saturation conditions),

$$\ln(p_{ws}) = \sum_{i=0}^{5} m_i T^{i-1} + m_6 \ln(T) \tag{4}$$

Table I provides the values of g_i and m_i. Details on the ITS-90 conversion are given in the Appendix.

For the real-gas mixture model, the humidity ratio w_r is defined by

$$w_r = \frac{M_w}{M_a} \frac{x_w}{x_a} = \frac{M_w}{M_a} \frac{x_w}{1 - x_w} \tag{5}$$

where x_w and x_a are water-vapor and dry air molar fractions, respectively.

The value of x_w stems from the definition of relative humidity, ϕ:

$$x_w = \phi x_{ws} \tag{6}$$

where the water-vapor saturation molar fraction $x_{ws}(T, P)$ is defined as [6]

$$x_{ws} = \frac{f p_{ws}}{P} \tag{7}$$

Specifically, the coefficient f occurring in Eq. (7) is a dimensionless quantity introduced by Goff [10], termed the enhancement factor. According to Hyland and Wexler [11],

Table I. Coefficients for the Relationships Used in the Program

	Eq. (3), g_i	Eq. (4), m_i	Eq. (10), j_i $(0 \leqslant t \leqslant 100°C)$	Eq. (10), j_i $(100 \leqslant t \leqslant 150°)$
-1	-0.579187×10^{4}	—	—	—
0	0.903455	-0.567753×10^{4}	0.50885×10^{2}	0.508783×10^{2}
1	-0.489267×10^{-1}	0.642619×10	0.616453	0.621676
2	0.419007×10^{-4}	-0.965145×10^{2}	0.146008×10^{-2}	0.139919×10^{-2}
3	-0.144607×10^{-7}	0.867159×10^{-6}	0.200973×10^{-4}	0.213950×10^{-4}
4	0.663969×10	0.125406×10^{-8}	-0.585084×10^{-7}	-0.712716×10^{-7}
5	—	$-0.213591 \times 10^{-12}$	0.410333×10^{-9}	0.462843×10^{-9}
6	—	0.415576×10	0.196769×10^{1}	0.197695×10^{-1}
7	—	—	—	—

	Eq. (15), F_i	Eq. (33), a_i	Eq. (33), d_i	Eq. (37), q_i
0	-0.239871×10^{4}	0.489741	-0.199798×10^{4}	-0.647556×10^{3}
1	-0.143481×10	0.288118×10^{2}	0.180357×10	0.273756
2	0.106854	0.187627×10^{-2}	0.364005×10^{-3}	0.291149×10^{-2}
3	-0.291493×10^{-3}	-0.765689×10^{-5}	-0.108149×10^{-5}	
4	0.373530×10^{-6}	0.141089×10^{-7}	0.287266×10^{-8}	0.107×10^{-5}
5	-0.212011×10^{-9}	$-0.695756 \times 10^{-11}$	0.175083×10^{-11}	—
6	-0.342060×10	—	—	—
7	0.161780×10^{-1}	—	—	—

	Eq. (39), L_i $(0 \leqslant t \leqslant 100°C)$	Eq. (40), N_i $(100 \leqslant t \leqslant 130\ C)$	Eq. (41), N_i $(130 \leqslant t \leqslant 200°C)$
0	-0.159600×10^{4}	-0.781718×10^{-1}	-0.781718×10^{-1}
1	0.959942×10	-0.758102×10	-0.758102×10
2	-0.241610×10^{-1}	0.454564×10^{-1}	0.454564×10^{-1}
3	0.477701×10^{4}	-0.780915×10^{-4}	-0.780915×10^{-4}
4	-0.353823×10^{-7}	0.502819×10^{-7}	0.502819×10^{-7}
5	-0.371047×10^{-1}	—	-0.535009×10^{-5}
6	-0.771783×10^{7}	—	—

$$
\begin{aligned}
\ln(f) = {} & \left[\frac{(1+k_{\mathrm{T}})(P-p_{\mathrm{ws}})-0.5\,k_{\mathrm{T}}(P^2-p_{\mathrm{ws}}^2)}{RT}\right]\bar{v}_{\mathrm{ws}} \\
& + \ln(1-c_{\mathrm{H-a}}x_{\mathrm{as}}P) + \left(\frac{x_{\mathrm{as}}^2 P}{RT}\right)B_{\mathrm{aa}} \\
& - \left(\frac{P-p_{\mathrm{ws}}-x_{\mathrm{as}}^2 P}{RT}\right)B_{\mathrm{ww}} + \left[\frac{x_{\mathrm{as}}^3 P^2}{(RT)^2}\right]C_{\mathrm{aaa}} \\
& - \left[\frac{3x_{\mathrm{as}}^2(1-x_{\mathrm{as}})\,P^2}{(RT)^2}\right]C_{\mathrm{aww}} \\
& - \left(\frac{2x_{\mathrm{as}}^2 P}{RT}\right)B_{\mathrm{aw}} + \left[\frac{3x_{\mathrm{as}}^2(1-2x_{\mathrm{as}})\,P^2}{2(RT)^2}\right]C_{\mathrm{aaw}} \\
& - \left[\frac{2x_{\mathrm{as}}^3(2-3x_{\mathrm{as}})\,P^2}{(R(T)^2}\right]B_{\mathrm{aa}}B_{\mathrm{aw}} \\
& - \left[\frac{(1+2x_{\mathrm{as}})(1-x_{\mathrm{as}})^2\,P^2-p_{\mathrm{ws}}^2}{2(RT)^2}\right]C_{\mathrm{www}} \\
& + \left[\frac{6x_{\mathrm{as}}^2(1-x_{\mathrm{as}})^2\,P^2}{(RT)^2}\right]B_{\mathrm{ww}}B_{\mathrm{aw}} \\
& - \left[\frac{x_{\mathrm{as}}^2(1-3x_{\mathrm{as}})(1-x_{\mathrm{as}})\,P^2}{(RT)^2}\right]B_{\mathrm{aa}}B_{\mathrm{ww}} \\
& - \left[\frac{2x_{\mathrm{as}}^2(1-x_{\mathrm{as}})(1-3x_{\mathrm{as}})\,P^2}{(RT)^2}\right]B_{\mathrm{aw}}^2 \\
& - \left[\frac{3x_{\mathrm{as}}^4 P^2}{2(RT)^2}\right]B_{\mathrm{aa}}^2 - \left[\frac{p_{\mathrm{ws}}^2-(1+3x_{\mathrm{as}})(1-x_{\mathrm{as}})^3\,P^2}{2(RT)^2}\right]B_{\mathrm{ww}}^2 \qquad (8)
\end{aligned}
$$

where R is the molar gas constant ($R = 8.31441\ 10^6\ \mathrm{Pa\cdot cm^3\cdot mol^{-1}\cdot K^{-1}}$); x_{as} is the dry-air molar fraction in saturation conditions, from Eq. (7),

$$x_{\mathrm{as}} = \frac{P - fp_{\mathrm{ws}}}{P} \qquad (9)$$

and k_{T} is the isothermal compressibility of water in equilibrium with its vapor expressed as Pa^{-1}. In the temperature range 273 to 423 K [12] and extending up to 473 K (see Table I for j_i),

$$k_{\mathrm{T}} = \frac{\sum_{i=1}^{5} j_i(T-273.15)^i}{1 + j_6(T-273.15)}\,10^{-11} \qquad (10)$$

For $T \leqslant 273.16$ K [13] we have

$$k_T = (8.87435 + 0.0165023T)\,10^{-11} \tag{11}$$

C_{H-a} is the Henry constant for dry air expressed as Pa^{-1}. Approximating dry air to a mixture composed only of oxygen and nitrogen, we have

$$\frac{1}{C_{H-a}} = \left(\frac{x_{O_2}}{C_{H-O_2}} + \frac{x_{N_2}}{C_{H-N_2}}\right) \tag{12}$$

assigning 0.22 and 0.78 to the molar fractions of O_2, x_{O_2}, and N_2, x_{N_2}, respectively [6]. The Henry constant for oxygen and nitrogen is determined using Himmelblau's equation [14]: for $T \geqslant 273.15$ K

$$\alpha[\log(C_H)]^2 + (\gamma\tau + \delta)\log(C_H) + (\beta\tau^2 + \varepsilon\tau - 1) = 0 \tag{13}$$

with $\tau = 1000/T$. The values of the α, γ, β, and ε coefficients for nitrogen and oxygen are given in Table II and C_H is identical to either C_{H-O_2} or C_{H-N_2}, depending on the coefficients used. For $T < 273.15$ K, C_{Ha} is identical to zero.

$\bar{V}_{ws}$ is the molar volume of either the liquid or the solid phase of water under saturation conditions, expressed as $\text{cm}^3 \cdot \text{mol}^{-1}$. Depending on the thermodynamic conditions, it can be obtained from the following relationship [5, 6], whose coefficients have been modified to make account of ITS-90.

For $173.15 \leqslant T \leqslant 273.16$ K,

$$\bar{V}_{ws} = 18015.28\,(0.107000 \times 10^{-2} + 0.250959 \times 10^{-7}T + 0.371871 \times 10^{-9}T^2) \tag{14}$$

and for $273.16 \leqslant T \leqslant 423.15$ K,

$$\bar{V}_{ws} = 18015.28\,\frac{\sum_{i=6}^{7} F_i T^{i-6}}{\sum_{i=0}^{5} F_i T^i} \tag{15}$$

where coefficients F_i are as given in Table I.

Table II. Coefficient for Calculating the Henry Constant

	Nitrogen	Oxygen
a	−0.1021	−0.0005960
b	−0.1482	−0.1470
g	−0.01894	−0.05143
d	−0.03773	−0.1084
e	0.8510	0.8447

The virial coefficients B_{aa} (B_{ww}) and C_{aaa} (C_{www}) in Eq. (8), expressed as $cm^3 \cdot mol^{-1}$ and $cm^6 \cdot mol^{-2}$, respectively, depend on temperature as follows.

For water,

$$B_{ww} = RT\left[0.702089 \times 10^{-8} - 0.147\text{-}008 \times 10^{-8} \exp\left(\frac{1734.636}{T}\right)\right] \quad (16)$$

$$C_{www} = (RT)^2 \left[0.1666295 \times 10^{-14} - 0.334522 \times 10^{-17} \exp\left(\frac{3645.78}{T}\right) + \left(\frac{B_{ww}}{RT}\right)^2\right] \quad (17)$$

and for dry air,

$$B_{aa} = 0.34938 \times 10^2 - \frac{0.666754 \times 10^4}{T} - \frac{0.210704 \times 10^7}{T^2} + \frac{0.928923 \times 10^8}{T^3} \quad (18)$$

$$C_{aaa} = 0.125995 \times 10^4 - \frac{0.191070 \times 10^6}{T} + \frac{0.63277 \times 10^8}{T^2} \quad (19)$$

The second and third interaction coefficients of air–water vapor mixtures, B_{aw}, C_{aww}, and C_{aaw}, as $cm^3 \cdot mol^{-1}$ and $cm^6 \cdot mol^{-2}$, respectively, are expressed as

$$B_{aw} = 0.323507 \times 10^2 - \frac{0.140969 \times 10^5}{T} - \frac{0.124837 \times 10^7}{T^2} - \frac{0.231946 \times 10^{10}}{T^4} \quad (20)$$

$$C_{aaw} = 0.482937 \times 10^3 + \frac{0.105546 \times 10^6}{T} - \frac{0.656519 \times 10^8}{T^2} + \frac{0.294612 \times 10^{11}}{T^3} - \frac{0.319531 \times 10^{13}}{T^4} \quad (21)$$

$$C_{aww} = -10^6 \exp\left(-0.10728 \times 10^2 + \frac{0.347663 \times 10^4}{T} - \frac{0.382954 \times 10^6}{T^2} + \frac{0.333743 \times 10^8}{T^3}\right) \quad (22)$$

The unknowns x_{as} and f can be determined from Eqs. (8) and (9) by iteration. In the first run, f is set to unity and x_{as} is derived accordingly. The iterations proceed until the solutions stabilize to within 10^{-8} of their value.

Figure 1 shows the values of the enhancement factor as the temperature and the total pressure of the mixture vary.

Alternatively, f can be calculated by means of the relationships proposed by Giacomo [15], in the 0 to 30°C and 60- to 110-kPa range, and by Aslam et al. [16], in the 55°C range and up to 50 MPa, introducing a deviation of, respectively, 0.1 and 0.5% with respect to the values calculated using Eq. (7).

2.2. Calculation of $w = w(P, T_d)$

The humidity ratio is obtained from the dew-point temperature T_d and the total pressure P on the basis of

$$w_s(P, T_d) = w(P, T) \tag{23}$$

Consequently for an ideal mixture, Eq. (2) becomes

$$w_i = \frac{M_w}{M_a} \frac{p_{ws}(T_d)}{P - p_{ws}(T^d)} \tag{24}$$

since $p_{ws}(T_d) = \phi p_{ws}(T)$, according to Dalton's law.

For a real mixture, one obtains on the basis of Eqs. (5) and Eq. (23),

$$w_r = \frac{M_w}{M_a} \frac{x_{ws}(P, T_d)}{1 - x_{ws}(P, T_d)} \tag{25}$$

where x_{ws} is related to T_d and P through Eq. (7).

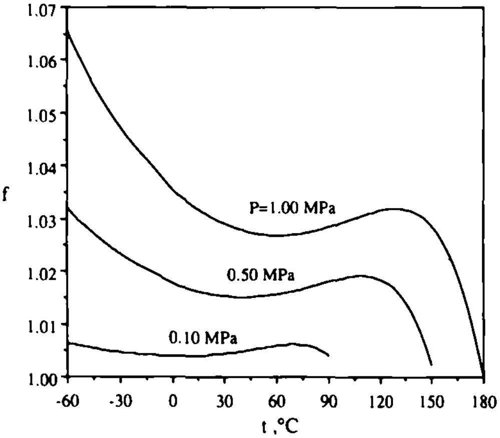

Fig. 1. Enhancement factor as the temperature and pressure vary.

2.3. Calculation of $w = w(P, T, T^*)$

Imposing the energy convervation for a moist air adiabatic saturation process, w is related to T^* as follows:

$$h(P, T, w) + [w_s(P, T^*) - w(P, T)]\, h_w(P, T^*) = h_s[P, T^*, w_s(P, T^*)] \tag{26}$$

In the case of an ideal mixture, w can be obtained by simplifying Eq. (26), i.e.,

$$w_i = \frac{[\Delta h_0 - (c_{pw} - c_{pv})\, t^*]\, w_s - c_{pa}(t - t_s^*)}{\Delta h_0 + c_{pv} t - c_{pw} t^*} \tag{27}$$

where w_s is calculated using the hypothesis of an ideal mixture; Δh_0 is the latent heat of vaporization (sublimation), namely, 2500.8 $\mathrm{J \cdot g^{-1}}$ for saturation conditions of liquid water and 2834.8 $\mathrm{J \cdot g^{-1}}$, in the case of ice; and c_{pa}, c_{pv}, c_{pl}, and c_{pi} are the constant-pressure specific heats, expressed as $\mathrm{J \cdot g^{-1}\,K}$ of dry air, of water vapor and the liquid and solid phases of water, respectively. They result as follows.

For $-100 \leqslant t \leqslant 200°\mathrm{C}$,

$$c_{pa} = 1.0044 - 2.18264 \times 10^{-6} t + 6.19428 \times 10^{-7} t^2 \tag{28}$$

for $t \leqslant 0°\mathrm{C}$,

$$c_{pv} = 1.845 \tag{29}$$

$$c_{pi} = 2.11598 + 0.00790171 t + 5.25804 \times 10^{-6} t^2 \tag{30}$$

and for $0 \leqslant t \leqslant 200°\mathrm{C}$,

$$c_{pv} = 1.845 - 5.80838 \times 10^{-2} t + 3.47902 \times 10^{-5} t^2 - 1.66303 \times 10^{-7} t^3 + 6.61315 \times 10^{-10} t^4 \tag{31}$$

$$c_{pl} = 4.21754 - 0.00154336 t + 0.0000148244 t^2 \tag{32}$$

To obtain w from Eq. (26) for a real mixture it is necessary to determine the specific enthalpy h of moist air expressed as $\mathrm{J \cdot g^{-1}}$ and related to temperature, total pressure, and molar fractions [6]:

$$h = \left[x_a \left(\sum_{i=0}^{5} a_i T^i - 7914.1982 \right) + x_w \left(\sum_{i=0}^{5} d_i T^i + 35994.17 \right) + RT \left(B_m - T \frac{bB_m}{dT} \right) \frac{1}{\bar{V}_m} + \left(C_m - \frac{1}{2} T \frac{dC_m}{dT} \right) \frac{1}{\bar{V}_m^2} \right] \frac{1}{M_a x_a} \tag{33}$$

with

$$B_m = x_a^2 B_{aa} + 2x_a x_w B_{aw} + x_w^2 B_{ww} \tag{34}$$

$$C_m = x_a^3 C_{aaa} + 3x_a^2 x_w C_{aaw} + 3x_a x_w C_{aww} + x_w^3 C_{www} \tag{35}$$

where the molar volume of the moist air mixture $\bar{V}_m$, expressed as $\mathrm{cm^3 \cdot mol^{-1}}$, is calculated using the virial equation truncated after the second term:

$$\frac{P\bar{V}_m}{RT} = 1 + \frac{B_m}{V\bar{P}_m} + \frac{C_m}{\bar{V}_m^2} \tag{36}$$

Equation (36) is solved proceeding with successive approximations until the right-hand and left-hand sides balance to better than 10^{-4} of their values. The coefficients a_i and d_i of Eq. (33) are given in Table I.

Assuming, to calculate h_s, that the specific enthalpy of pure compressed liquid water (ice) h_w, expressed as $\mathrm{J \cdot g^{-1}}$, at temperature T^*, is approximately equal to the enthalpy of saturated liquid water (saturated ice) at the same temperature, h_{ws}; i.e., for $T \leqslant 273.16$ K,

$$h_w = h_{ws} = \sum_{i=0}^{3} q_i T^i + q_4 p_{ws} \tag{37}$$

and for $273.16 \leqslant T \leqslant 373.125$ K,

$$h_w = h_{ws} = \chi(T) - 0.01214 + T\bar{V}_{ws} \frac{dp_{ws}}{DT} \frac{1}{18015.28} \tag{38}$$

where α, expressed as $\mathrm{J \cdot g^{-1}}$, can be calculated.

For $273.16 \leqslant T \leqslant 373.127$ K,

$$\chi = \sum_{i=0}^{4} L_i T^i + L_5\, 10^{L_6(T-273.15)} \tag{39}$$

for $373.125 \leqslant T \leqslant 403.128$ K,

$$\chi = \sum_{i=0}^{4} N_i T^i \tag{40}$$

and for $403.128 \leqslant T \leqslant 473.15$ K,

$$\chi = \sum_{i=0}^{4} N_i T^i = N_5 (T - 403.128)^{3.1} \tag{41}$$

and the values of coefficients L_i, q_i, and N_i are given in Table I.

The humidity ration w_s is determined through Eq. (7) from the thermodynamic wet bulb temperature, T^*, and the total pressure.

Equation (26) is solved iteratively since Eqs. (33)–(35) contain the unknown variable x_w. The value of the first attempt can be obtained from Eq. (27), which is valid assuming the ideal mixture, and from Eq. (4). In the algorithm the solution is acceptable when the difference in absolute value between the left and the right side of Eq. (26) is less than $10^{-4}\ \mathrm{J \cdot g^{-1}}$.

2.4. Calculation of $\phi = \phi(P, T, w)$

Assuming an ideal mixture, it is

$$\phi_i = \frac{wP}{p_{ws}(w + M_w/M_a)} \tag{42}$$

For a real mixture, we have

$$\phi_r = \frac{x_{ws}(P, T_d)}{x_{ws}(P, T)} \tag{43}$$

where x_w is derived from w through Eq. (5) and x_{ws} from T and P through Eq. (7).

2.5. Calculation of $\phi = \phi(P, T_d, T)$

For an ideal mixture one has

$$\phi_i = \frac{p_{ws}(T_d)}{p_{ws}(T)} \tag{44}$$

whereas, for a real mixture, ϕ is related to P, T, and T_d through Eq. (7) and the following equation:

$$\phi_r = \frac{x_{ws}(P, T_d)}{x_{ws}(P, T)} \tag{45}$$

2.6. Calculation of $\phi = \phi(P, T, T^*)$

For an ideal mixture the value of the relative humidity is calculated using Eq. (39) and obtaining the humidity ratio from Eq. (27); for a real mixture it is calculated applying Eq. (43) and obtaining the values of x_w from Eqs. (26)–(41) and x_{ws} from Eq. (6).

3. RESULTS

The aim of this study is to establish how far the ideal-mixture model can be used as a sufficient approximation for moist air in the 0.1- to 1-MPa total pressure range and in the −60 to 180°C temperature range. Such a problem does not lend itself to a unique solution, but instead a choice between the ideal-mixture and the real-mixture models can be made exclusively for a particular case and application. Thus, to let the readers draw their conclusions, the results of the comparisons between the two models for the previously examined cases (2.1–2.6) are reported in the same order below. To simplify the comparison, the subranges where the derviations as defined by Eq. (1) are within 2% or, alternatively, 4% are highlighted wherever applicable.

3.1. Calculation of $w = w(P, T, \phi)$

Figure 2 shows the values of the relative differences in humidity ratio as related to relative humidity and temperature, for different values to total pressure. It can be noted that, for equal temperatures above 0°C, the relative difference, s_w, increases monotonically with ϕ, always attaining the highest value under saturation conditions. For temperatures below 0°C, s_w is independent of ϕ. For a constant relative humidity, s_w is a nonmonotonic function of t. Keeping t and ϕ constant, s_w increases with pressure.

At atmospheric pressure (Fig. 2), in the −60 to 90°C temperature range, the relative difference is less than 1.3% up to 90°C.

At a pressure of 0.5 MPa, s_w does not exceed 2% between −10 and 90°C and 4% in the whole temperature range examined. However, at a pressure of 1 MPa, only between −20 and 120°C is s_w less than 4%.

3.2. Calculation of $w = w(P, T_d)$

This case does not require a specific analysis as the relevant results can always be derived from those in Section 3.1 assuming saturation conditions.

3.3. Calculation of $w = w(P, T, T^*)$

Not with standing the measurement difficulty of T^*, the analysis of case 3.3 brings to light some significant theoretical results. In Fig. 3, the trace for each temperature terminates when the humidity ratio increases to the saturation value. From Fig. 3 one can immediately conclude that, for $t < 20$°C, s_w always reaches its minimum under saturation conditions. Furthermore, this statement holds true for higher temperatures as the pressure increases, e.g., 40°C at 0.5 MPa and 80°C at 1 MPa.

As t increases above those limits, the minimum gradually moves toward w values which are lower than w_s. On the contrary, the maximum value is always reached under dry-air conditions, where the relative difference tends toward infinity. Hence, the ideal model for dry mixtures should be adopted with caution since the derviation between the two models can sometimes lead to intolerable uncertainties. It is worth noting that even when the thermodynamic wet-bulb temperature is approximated with the wet-bulb temperature given by a good psychrometer, one encounters the same difficulty again since this instrument does not provide

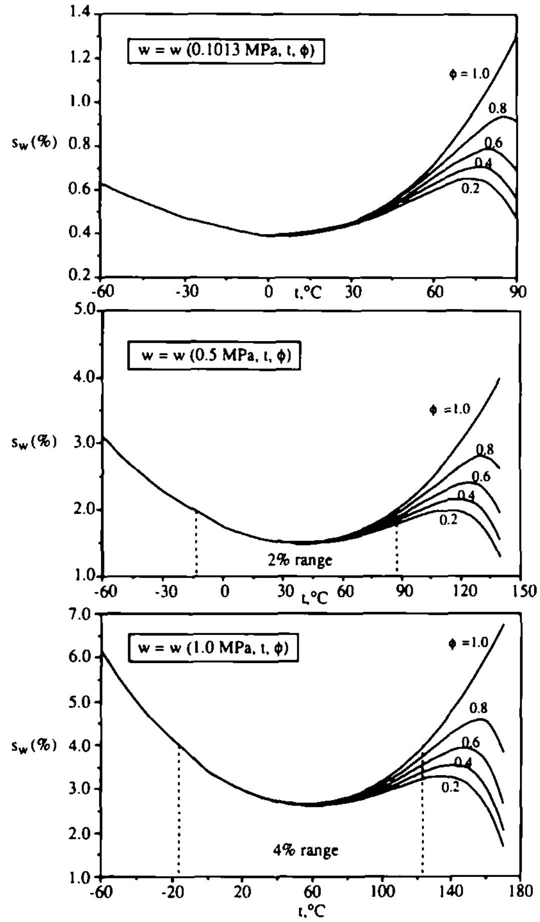

Fig. 2. Trend of the humidity-ratio relative differences as the temperature and the relative humidity vary.

accurate measurements with dry air. For this reason, Fig. 3 provides s_w up to a value corresponding to a ϕ value to 30%. Furthermore, it is rather unlikely that the psychrometer can be operated with $t < 0^\circ C$.

At atmospheric pressure, s_w does not exceed 5% for $0 \leqslant t \leqslant 80^\circ C$. At 20°C, s_w varies between 0.5 and 3%. This is a much worse result than those in Fig. 2. And the higher the pressure, the worse the result, as one can see from Fig. 3. It may then be concluded that it is more advisable to derive w from the measurement of ϕ and t or, preferably, of t_d and t, rather than from dry- and wet-bulb measurements.

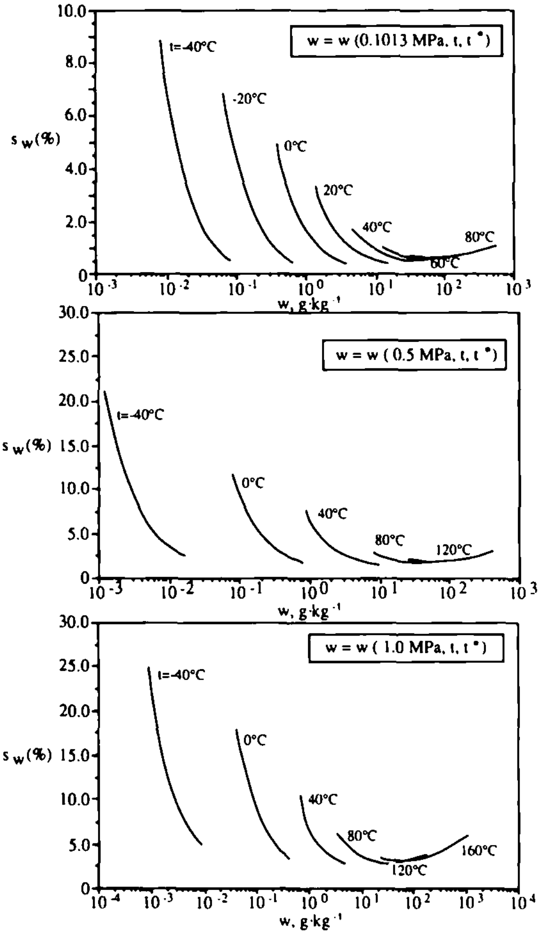

Fig. 3. Trend of the humidity-ratio relative differences as the humidity ratio and the temperature vary.

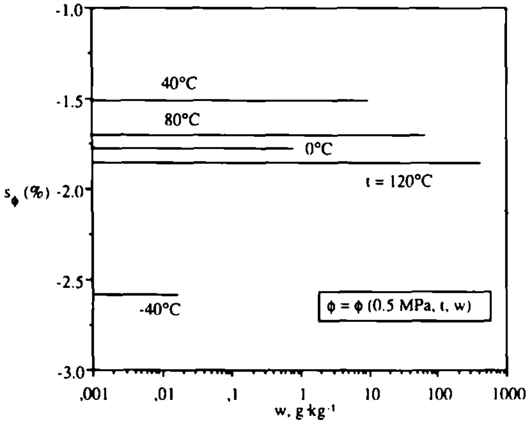

Fig. 4. Trend of the relative-humidity relative differences as the humidity ratio and the temperature vary at a pressure of 0.5 MPa.

3.4. Calculation of $\phi = \phi(P, T, w)$

Having made the quite obvious assumption that for dry air s_ϕ is identical to zero since $\phi = 0$, one can obtain more interesting information from Fig. 4. It is interesting to note that s_ϕ does not depend on w if t and p are constant. It depends on t in a nonmonotonic fashion as a consequence of $f(t)$ (see Fig. 1). Furthermore, and with reference to Fig. 5, one can

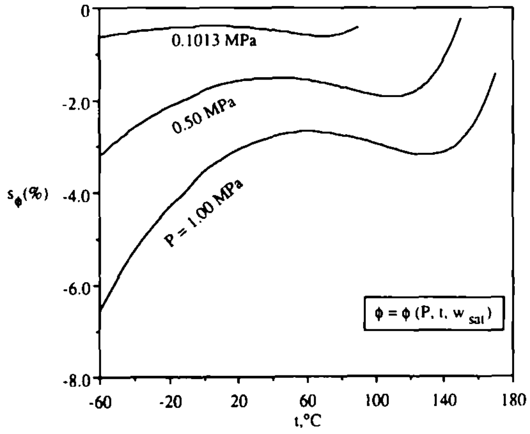

Fig. 5. Trend of the relative-humidity relative differences as the temperature and the pressure vary under saturation conditions.

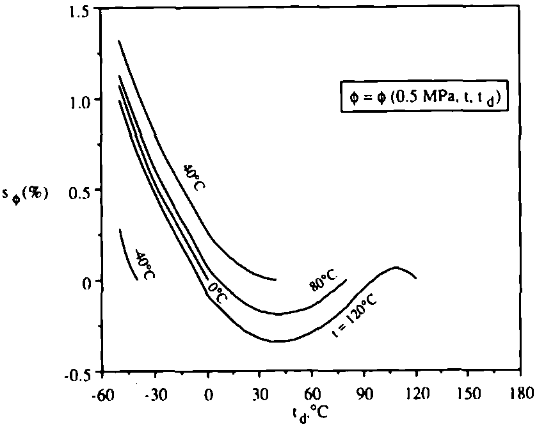

Fig. 6. Trend of the relative-humidity relative differences as the dew-point and air temperatures vary at a pressure of 0.5 MPa.

see that the *t* dependence is about the same at different pressures. At atmospheric pressure, s_ϕ is nearly constant, ranging from -0.4 to 0.6%. At 0.5 MPa, s_ϕ ranges between 0 and 2% for $-10 \leqslant t \leqslant 140$°C, with a minimum of -3.2% in the whole range. Final, at la MPa the absolute deviations are much larger and increase quickly as *t* decreases below 60°C.

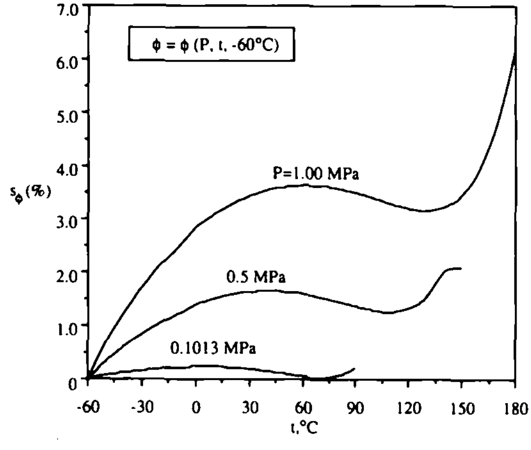

Fig. 7. Trend of the relative-humidity relative differences as the air temperature and the pressure vary at a dew-point temperature of -60°C.

3.5. Calculation of $\phi = \phi(P, T_d, T)$

The results of the comparison between the ideal-gas and the real-gas approaches to evaluate ϕ in relation to t, t_d, and P are examined in Figs. 6 and 7.

From Fig. 6 it is evident that s_ϕ depends in a nonmonotonic fashion on both t_d and t; this behavior can again be explained by the relation of the enhancement factor to temperature. A maximum difference of 1.3% is found at the lowest dew point considered.

For that dew-point temperature, Fig. 7 shows the dependence on pressure and air temperature: s_ϕ increases with pressure and exhibits a

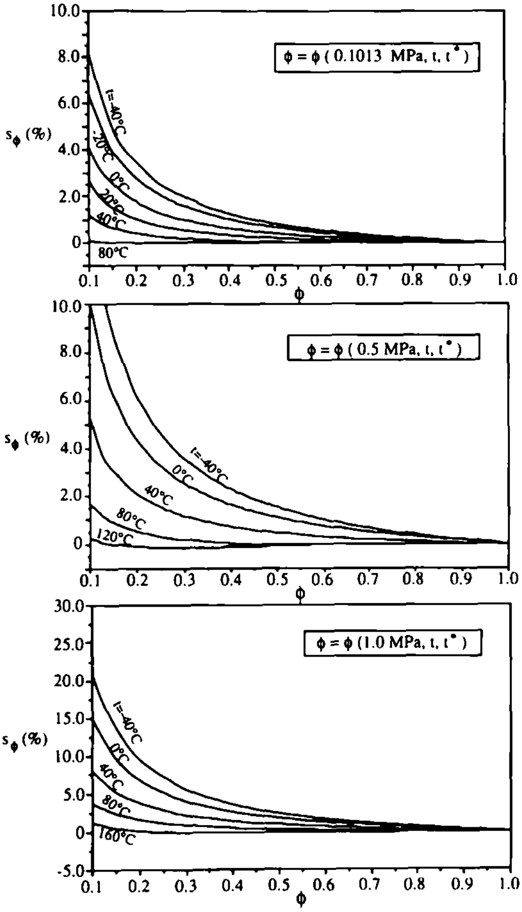

Fig. 8. Trend of the relative-humidity relative differences as the relative humidity and the temperature vary.

behavior traceable to that of the enhancement factor at high temperatures. Then, considering that all cases with $t \geqslant 0°C$ are quite uncommon and, probably, completely unrealistic, the maximum practical difference does not exceed 3%.

3.6. Calculation of $\phi = \phi(P, T, T^*)$

To determine ϕ from t, t^*, and P presents evident analogies with the previously examined case 3.3. Specifically, s_ϕ reaches its minimum under the same conditions as s_w in case 3.3 and tends to infinity for dry-air conditions.

As highlighted for case 3.3, Fig. 8 shows the differences, s_ϕ, in relation to t and to ϕ for three absolute pressures: ϕ spans the range 0.1 to 1.

As could be expected, the s_ϕ curves tend to diverge as ϕ approaches 0.1 and, then, 0, and the lower the air temperature, the greater the divergence. However, the higher the air temperature, the closer is the ideal-gas model to the real-gas one. It is worth noting that $t = 80°C$, $P = 0.1$ MPa, and $t = 120°C$, $P = 0.5$ MPa, are two conditions with almost-negligible s_ϕ values.

4. CONCLUSIONS

The approximate errors yielded by an ideal-gas approach when dealing with mixtures of air and water vapor have been estimated by means of a comparison with a real-gas model for the same mixtures. The results have been expressed in terms of percentage deviations of humidity ratio, w, and relative humidity, ϕ, from the real case.

New basic equations describing the water thermodynamic equilibria [see Eqs. (2) and (3)] and the real-gas model have been introduced on the ground of the new International Scale of 1990, ITS-90. The scale conversion, as described in the Appendix, was performed on the numerical equations available in the literature with a sufficient degree of numerical accuracy. It still remains to determine whether a refitting of the original experimental data with ITS-90 conversion could yield a significantly better result.

At atmospheric pressure, ϕ and w can be derived with either model from direct measurements of either w or T_d and of either ϕ or T_d, respectively, in the air temperature range -60 to 90°C. Only when an accuracy better than 1.5%, or better then 0.6% in the case of $\phi(w)$, is sought is it necessary to introduce the real-mixture model.

When ϕ or w is derived from the thermodynamic wet-bulb temperature, a substantially different situation results: In most cases the differences exceed 3%. Smaller deviations occur for $t \geqslant 20°\text{C}$ and at atmospheric pressure. Low water-vapor concentrations are determined with a relatively poor accuracy using an ideal-gas approach. At pressures higher than atmospheric, the situation may become intolerably worse.

On the other hand, the psychrometric approach based on the ideal-mixture model produces good results for air temperatures between 60 and 80°C from the saturation temperature. In such a case and at atmospheric pressure, s_ϕ does not exceed 1% does not exceed 1% for $\phi \geqslant 0.25$. It is worth noting that a practical psychrometer should produce, by general consensus, reliable results in the range of from 0.25 to 0.95.

Final, the calibration of the relative humidity scales of hygroscopic hygrometers as well as the determination of ϕ by means of dew-point hygrometers are quite often carried out on the grounds of Eq. (43). In this light, $s_\phi(T_d)$, as shown in Figs. 6 and 7, is of great importance to humidity metrology.

APPENDIX

The thermodynamic relationships used in this study have been appropriately modified in the light of the corrections introduced by the ITS-90 with respect to the IPTS-68. A numerical approach was used (i) initially, to correct T_{68} in relation to the corresponding value of T_{90} [17] using

$$(T_{90} - T_{68}) = \sum_{i=1}^{8} b_i \left(\frac{T_{90} - 273.15}{630} \right)^i \tag{A1}$$

which is valid in the range 73.15 to 903.75 K, and (ii) to calculate the thermodynamic properties using the existing relationships in the literature for T_{68}. The coefficients of Eq. (A1) are

$b_1 = -0.148759$, $b_2 = -0.267408$, $b_3 = 1.080760$, $b_4 = 1.269056$

$b_5 = -4.089591$, $b_6 = -1.871251$, $b_7 = 7.438081$, $b_8 = -3.536296$

Furthermore, and for greater completeness, the thermodynamic relationships in question were re-evalued in their respective validity ranges. This re-evaluation was carried out keeping the structure of the relationship formally identical to that in the literature and determining the new coefficients using either a linear regression method or the Levenberg–Marquant method for nonlinear regressions, depending on the case.

Table AI compares the maximum deviation of every particular relationship on T_{68} from the corresponding T_{90} relationship with the maximum

Table AI. Comparison Between T_{68} and T_{90} Relationships

Eq.	Relationship	Maximum deviation from T_{68}	Maximum residual of T_{90} fitting
(2)	P_{ws} $(273.16 \leqslant T \leqslant 473.15\ \mathrm{K})$	8.3×10^{-4}	1.4×10^{-7}
(3)	P_{ws} $(173.15 \leqslant T \leqslant 273.16\ \mathrm{K})$	2.8×10^{-3}	7.8×10^{-10}
(9)	K_T $(373.15 \leqslant T \leqslant 423.15\ \mathrm{K})$	4.0×10^{-4}	2.1×10^{-4}
(9)	K_T $(273.15 \leqslant T \leqslant 373.15\ \mathrm{K})$	1.8×10^{-4}	9.1×10^{-5}
(10)	K_T $(T \leqslant 273.15\ \mathrm{K})$	1.9×10^{-5}	2.7×10^{-6}
(12)	$C_{\mathrm{H-O_2}}$	2.6×10^{-10}	1.3×10^{-10}
(12)	$C_{\mathrm{H-N_2}}$	7.1×10^{-6}	3.6×10^{-6}
(14)	V_{ws} $(173.15 \leqslant T \leqslant 273.16\ \mathrm{K})$	1.4×10^{-6}	3.0×10^{-8}
(15)	V_{ws} $(273.16 \leqslant T \leqslant 423.15\ \mathrm{K})$	7.2×10^{-5}	3.6×10^{-6}
(18)	B_{aa}	9.9×10^{-3}	2.8×10^{-4}
(19)	C_{aaa}	0.25	0.011
(20)	B_{aw}	0.11 %	0.0069 %
(21)	C_{aaw}	0.0075 %	1.9×10^{-4} %
(22)	C_{aww}	0.11 %	0.0052 %

value of the residuals produced in the T_{90} fitting. Unless specified differently, the deviations and residuals are given as the ratio to the appropriate value.

On the grounds of these differences, the correction of the relationship to account for the ITS-90 is, in general, of quite limited practical importance, in particular when considering the current measurement accuracy. According to Table AI, using uncorrected relationship causes errors of the order of magnitude of 10^{-3}. The coefficients in Table AI provide redundant accuracy to ease calculations.

The correction of the coefficients in Eqs. (18) through (22) is redundant as well, although theoretically correct. The relevant experimental relationships have a sensibly lower accuracy.

NOMENCLATURE

Δh_0	Latent heat of vaporization
ϕ	Relative humidity
ϕ_i	Ideal relative humidity
ϕ_r	Real relative humidity
B_{aa}	Second dry-air virial coefficient
B_{aw}	Second moist-air interaction virial coefficient
B_m	Second mixture virial coefficient
B_{ww}	Second water-vapor virial coefficient
C_{aaa}	Third dry-air virial coefficient

C_{aaw}	Third Moist-air interaction virial coefficient
C_{aww}	Third moist-air interaction virial coefficient
C_{H-a}	Henry's constant for moist air
C_{H-O_2}	Henry's constant for oxygen
C_{H-N_2}	Henry's constant for nitrogen
C_m	Third mixture virial coefficient
c_{pa}	Specific heat of constant-pressure dry air
c_{pi}	Specific heat of constant-pressure solid water
c_{pv}	Specific heat of constant-pressure water vapor
c_{pl}	Specific heat of constant-pressure liquid water
B_{ww}	Third virial coefficient of the water vapor
f	Enhancement factor
h	Specific enthalpy of moist air
h_w	Specific enthalpy of water
h_{ws}	Specific enthalpy of water under saturation conditions
k_T	Compressibility coefficient of isothermic water
m_w	Mass of water vapor
m_a	Mass of air
M_a	Molecular weight of air
M_w	Molecular weight of water
P	Total pressure of moist air
p_w	Partial pressure of water vapor in moist air
p_{ws}	Pressure of saturated pure water
R	Universal gas constant
s_ϕ	Relative difference of the relative humidity
s_w	Relative difference of the humidity ratio
t, T	Air temperature (°C, K)
t_d, T_d	Dew-point temperature (°C, K)
t^*, T^*	Thermodynamic wet-bulb temperature (°C, K)
$\bar{V}_m$	Molar volume of moist air
$\bar{V}_{ws}$	Molar volume of water under saturation conditions
w	Humidity mixing ratio
w_i	Ideal humidity mixing ratio
w_r	Real humidity mixing ratio
w_s	Humidity mixing ratio under saturation conditions
x_a	Molar fraction of dry air
x_{as}	Molar fraction of dry air under saturation conditions
x_w	Molar fraction of water
x_{ws}	Molar fraction of water under saturation conditions

REFERENCES

1. L. P. Harrison, in *Humidity and Moisture Measurement and Control in Science and Industry, Vol. III* (Reinhold, New York, 1965), pp. 3–69.
2. J. L. Threlked, *Thermal Environmental Engineering* (Prentice Hall, New York, 1970), p. 175.
3. R. M. Nelson and M. Pate, *ASHRAE Trans.* **89**(2):435 (1986).
4. L. Crovini, A. Actis, A. Carotenuto, M. Dell'Isola, and P. Vigo, Accurate Solutions to Humidity Measurement Problems, *Proc. 13th IMEKO*, Torino (1994).
5. R. W. Hyland and A. Wexler, *Trans. ASHRAE* **89**(2):520 (1983).
6. R. W. Hyland and A. Wexler, *Trans. ASHRAE* **89**(2):500 (1983).
7. American Society of Heating, Refrigeration, and Air-Conditioning Engineers, *ASHRAE Handbooks Fundamentals* (ASHRAE, Atlanta, 1993), pp. 6.1–6.17.
8. H. Preston-Thomas, *Metrologia* **27**:3 (1990).
9. A. Carotenuto, M. Dell'Isola, and P. Vigo, *Trans. Measure. Control* (1994), in press.
10. J. A. Goff, *Piping Air Condition.* **21**:118 (1949).
11. R. W. Hyland and A. Wexler, *J. Res. NBS* **77A**:133 (1973).
12. G. S. Kelly, *J. Chem. Eng.* **20**:97 (1975).
13. A. J. Leadbetter, *Proc. Roy. Soc.* **A287**:124 (1965).
14. D. M. Himmelblau, *J. Chem. Eng. Data* **5**:35 (1960).
15. P. Giacomo, *Metrologia* **18**:33 (1982).
16. S. Aslam, M. Charmchi, and R. A. Gaggioli, *ASHRAE Trans.* **86**(10):448 (1986).
17. R. N. Goldberg and R. D. Weir, *Pure Appl. Chem.* **64**:1545 (1992).